Design and characterization of a cleavage-resistant Annexin A1 mutant to control inflammation in the microvasculature

Magali Pederzoli-Ribeil,[1] Francesco Maione,[1] Dianne Cooper,[1] Adam Al-Kashi,[1] Jesmond Dalli,[1] *Mauro Perretti,[1] and *Fulvio D'Acquisto[1]

[1]William Harvey Research Institute, Barts and The London School of Medicine, Queen Mary University of London, London, United Kingdom

Human polymorphonuclear leukocytes adhesion to endothelial cells during the early stage of inflammation leads to cell surface externalization of Annexin A1 (AnxA1), an effector of endogenous anti-inflammation. The antiadhesive properties of AnxA1 become operative to finely tune polymorphonuclear leukocytes transmigration to the site of inflammation. Membrane bound proteinase 3 (PR3) plays a key role in this microenvironment by cleaving the N terminus bioactive domain of AnxA1. In the present study, we generated a PR3-resistant human recombinant AnxA1—named super-AnxA1 (SAnxA1)—and tested its in vitro and in vivo properties in comparison to the parental protein. SAnxA1 bound and activated formyl peptide receptor 2 in a similar way as the parental protein, while showing a resistance to cleavage by recombinant PR3. SAnxA1 retained anti-inflammatory activities in the murine inflamed microcirculation (leukocyte adhesion being the readout) and in skin trafficking model. When longer-lasting models of inflammation were applied, SAnxA1 displayed stronger anti-inflammatory effect over time compared with the parental protein. Together these results indicate that AnxA1 cleavage is an important process during neutrophilic inflammation and that controlling the balance between AnxA1/PR3 activities might represent a promising avenue for the discovery of novel therapeutic approaches. (*Blood*. 2010;116(20):4288-4296)

Introduction

The initial phase of an inflammatory response is characterized by the recruitment and activation of circulating polymorphonuclear leukocytes (PMNs) to the site of inflammation. During this phase, neutrophils egress the vascular endothelium and migrate into peripheral tissues thanks to the coordinated action of adhesion molecules and other mediators, including proinflammatory cytokines and autacoids.[1] It is now appreciated that elicitation of this inflammatory cascade leads also the activation of counter-regulatory pathways to contain these responses, ensuring that resolution of inflammation takes place once the dangerous stimulus has been disposed of.[2,3] Among these effectors of resolution there is the Annexin A1 (AnxA1)–formyl peptide receptor 2 (FPR2) pathway, an endogenous homeostatic anti-inflammatory system[4] that acts as a "brake" for PMN adhesion to the microvascular wall preventing further cell transmigration to the inflammatory site.[5] This phenomenon occurs after the externalization of the protein to the cell surface where it binds to its cognate receptor FPR2,[6] initiating a cascade of signaling events eventually leading to rapid and late responses, including detachment of adherent cells,[7] L-selectin shedding,[8] and phagocytosis of apoptotic cells[9] (reviewed in[4]).

In analogy with the complexity—yet tight regulation—of the phenomena described above, the anti-inflammatory and antiadhesive effects of AnxA1 are also subjected to fine modulation; externalization of the protein on the PMN plasma membrane is accompanied by cleavage of a unique region[10] of the protein: the N terminus.[11] This region has been suggested to play a pivotal role for anti-inflammatory properties of the full-length protein and peptides designed on this 50-amino acid–long sequence display anti-inflammatory and tissue-protective properties.[7,12,13]

The cleavage of AnxA1 N terminus occurs after PMN activation[5] and has been extensively documented in vitro and in in vivo models of inflammation, as well as in human and experimental inflammatory exudates.[14,15] However, one point yet to be addressed is the functional relevance of AnxA1 cleavage upon PMN activation, with 2 alternative explanations: (1) AnxA1 cleavage is an homeostatic mechanism limiting the biologic function of the protein or (2) it is an activating step leading to the release of bioactive N terminus–derived peptidomimetics, so that the protein might act as a pro-drug.

We have recently addressed the issue of AnxA1 cleavage in the context of PMN activation, reporting a central role of proteinase 3 (PR3).[11] This enzyme is one of the PMN serine proteases,[16] and it is expressed both in PMN granules and membranes, contributing to the bactericidal and proinflammatory properties of these cells. Most interestingly, we found that PR3 colocalizes with AnxA1 after PMN activation and it becomes responsible for cleaving the protein at 3 discrete sites: Alanine[11], Valine[22], and Valine[36]. Thus, we hypothesized that blocking AnxA1 cleavage by PR3 would significantly affects its anti-inflammatory effects.

In this study, we have conducted a systematic analysis of the functional role of these 3 cleavage sites for susceptibility to PR3. Generation of a PR3 cleavage-resistant AnxA1 triple-mutant (AnxA1-$A^{11}R/V^{22}K/V^{36}K$, termed super AnxA1 or SAnxA1) was then accomplished, together with its in vitro and in vivo biologic characterization. We conclude that pharmacologic modulation of AnxA1 cleavage might represent a novel therapeutic strategy to limit excessive inflammatory responses.

Submitted February 16, 2010; accepted July 25, 2010. Prepublished online as *Blood* First Edition paper, August 12, 2010; DOI 10.1182/blood-2010-02-270520.

The publication costs of this article were defrayed in part by page charge payment. Therefore, and solely to indicate this fact, this article is hereby marked "advertisement" in accordance with 18 USC section 1734.

*M.P. and F.D. share senior authorship.

Methods

Cells

The stably transfected FPR2-HEK293 cell line was cultured as before.[17] PMNs of healthy individuals were isolated by Hystopaque (Sigma-Aldrich) sedimentation of blood collected in 3.2% sodium citrate (Sigma-Aldrich) as described[17] (experiments were approved by the Queen Mary University of London Research Ethics Committee; P/00/029 ELCHA). For preparation of whole cell lysates, PMNs and HEK293 cells were resuspended (1×10^8/mL and 2×10^6/mL, respectively) in lysis buffer (200mM NaCl, 20mM Tris-HCl, pH 8.0, 1% Triton X-100) for 10 minutes. When cell lysates were prepared for Western blot analysis only, a mixture of protease and phosphatase inhibitors was added to the lysis buffers.

Mice

Female BALB/c mice (7-8 weeks) or male C57BL/6 (23-28 g; Charles River) were kept under standard conditions and maintained in a 12-hour/12-hour light/dark cycle at 22°C in accordance with United Kingdom Home Office regulations (Guidance on the Operation of Animals, Scientific Procedures Act 1986) and of the European Union directives.

Molecular and cellular analyses

Site-directed mutagenesis. AnxA1 mutants were constructed by polymerase chain reaction mutagenesis using the double-tagged (c-Myc on the N terminus, Flag on the C-terminus, MFAnxA1) human AnxA1-pcDNA3.1[11] as a template. All mutants were constructed using oligonucleotide-mediated mutagenesis (QuickChange site-directed mutagenesis kit; Stratagene, Agilent Technologies UK Limited) according to the manufacturer's instructions. The single point mutations $A^{11}R$, $V^{22}K$, and $V^{36}K$ were constructed using oligonucleotides designed with QuickChange Primer Design Program. In addition to the single point mutations, 3 double-mutants ($A^{11}R/V^{22}K$, $A^{11}R/V^{36}K$, $V^{22}K/V^{36}K$) and one triple-mutant ($A^{11}R/V^{22}K/V^{36}K$) were also constructed. The oligonucleotide primers (0.4μM) were extended by PCR (19 cycles of consisting of incubation for 20 seconds at 95°C, 30 seconds at 55°C, and 14 minutes at 68°C) and final extension (10 minutes at 68°C) using Pfu Ultra DNA Polymerase (Promega) in presence of 5% dimethyl sulfoxide (Sigma-Aldrich). PCR products were digested using *Dpn*I (New England Biolabs) at 37°C for 2 hours and transformed into TOP10 cells (Invitrogen). The presence of each point mutation was confirmed by plasmid DNA sequencing (Cogenix).

Transfection. MFAnxA1 and MFAnxA1 mutants constructs (2 μg) were transfected into HEK293 cells, using 6 μL FuGENE6 transfection reagent (Roche) and 92 μL OptiMEM (Invitrogen) culture medium for each well of a 6-well culture plate (containing 5×10^5 cells). After 24 hours, cells from each well were lysed in 500 μL lysis buffer.

Western blotting. Samples boiled in 6 × Laemmli buffer were subjected to standard sodium dodecyl sulfate polyacrylamide gel electrophoresis and electrophoretically blotted onto polyvinylidene diflouride membranes (Millipore). Membranes were incubated with primary antibodies in Tris-buffered saline solution containing Tween 20 and 5% (wt/vo;) nonfat dry milk overnight before a 1.5-hour incubation period with horseradish peroxidase-conjugated secondary antibody (Dako). Proteins were detected using the enhanced chemiluminescence detection kit and visualized on Hyperfilm (Amersham Biosciences). The primary antibodies used were rabbit polyclonal anti-AnxA1 (Zymed Laboratories, Invitrogen), mouse monoclonal anti–c-Myc (Santa Cruz Biotechnology), mouse monoclonal anti-FLAG M2 (Sigma-Aldrich), and mouse monoclonal anti-phospho Erk1/2 and anti-Erk1/2 (Santa Cruz Biotechnology).

AnxA1 cleavage assay. All extracts used in the cleavage assay were prepared in the absence of proteases inhibitors. MFAnxA1 and MFAnxA1 mutant-transfected HEK293 cell lysates (150 μL) were immunoprecipitated with 10 μL anti–c-Myc antibody and 30 μL of protein G sepharose beads (Invitrogen), overnight at 4°C, in a final volume of 500 μL of lysis buffer. Same protocol was used to immunoprecipitated purified glutathione S-transferase (GST)–AnxA1 and GST-SAnxA1, using 50 μL glutathion sepahrose 4B beads (Amersham Biosciences). Purified PR3 (50-200 mU; Elastin Products) or neutrophil lysate were added to the immunoprecipitated product containing intact MFAnxA1 or MFAnxA1 mutants, or GST-AnxA1, or GST-SAnxA1. The reaction was incubated at 37°C for 30 minutes, and thereafter a mixture of protease inhibitors was added to prevent further proteolysis. The remaining pellet was boiled in 30 μL 6 × Laemmli buffer, and samples were subjected to 12% sodium dodecyl sulfate polyacrylamide gel electrophoresis.

Recombinant protein purification. AnxA1 wild-type and SAnxA1 (super AnxA1; triple mutant $A^{11}R/V^{22}K/V^{36}K$) were generated using pcDNA3.1/MFA1 and pcDNA3.1/MFA1-$A^{11}R/V^{22}K/V^{36}K$ as template. PCR (35 cycles of consisting of incubation for 1 minute at 94°C, 1 minute at 55°C, and 1 minute 20 seconds at 72°C) products were cloned into the *Bam*HI and *Xho*I sites of pGEX-6P-1 vector (GE Healthcare). BL21 *Escherichia coli* cells were transformed with pGEX-6P-1/AnxA1 or pGEX-6P-1/AnxA1-$A^{11}R/V^{22}K/V^{36}K$ mutant and grown overnight at 37°C under continues agitation (225 rpm). AnxA1 and SAnxA1 expression were induced incubating subconfluent culture (optical density, ~ 0.4) with 1mM IPTG (isopropyl β-D-1-thiogalactopyranoside; Promega) for an additional 6 hours at 37°C. Cell pellets from 1 L culture were lysed in 50 mL phosphate-buffered saline (PBS) containing 0.2% NP40, 1mM DTT, 5 mg DNase, 5 mg lysozyme and protease inhibitor cocktail (Roche) for 30 minutes, before loading onto a Glutathione Sepharose 4B column (GSTPrep FF; GE Healthcare) using an ÄKTAprime plus system along manufacturer's instruction. GST tag removal was carried out by loading 330 U PreScission protease (GE Healthcare). After overnight incubation at 4°C, recombinant proteins were eluted with phosphate buffer (140mM NaCl, 2.7mM KCl, 10mM Na_2HPO_4, and 1.8mM KH_2PO_4) and then dialyzed 5 times against PBS to remove any contaminant. The level of endotoxin were measured by the E-Toxate kit (Sigma-Aldrich) according to the manufacturer's instruction and were below 0.1 EU/mL. Protein concentration was determined using BCA protein assay kit (Pierce, Thermo Fisher Scientific, Perbio Science UK, Ltd). Proteins were stored at −80°C in PBS containing 5% glycerol.

In vitro analyses for bioactivity

Receptor binding assay. Receptor competition binding studies were performed on FPR2 stably transfected HEK293 cells as previously described.[17] Briefly, W-peptide (WKYMV; Phoenix Pharma) was iodinated on tyrosin (specific activity of 1507.17 Ci/mmol) and used as tracer. Cells (1×10^6) were incubated with 1μM cold W-peptide or increasing concentration of AnxA1 or SAnxA1 (1nM to 30μM) for 1 hour in Dulbecco PBS at 4°C. The bound and unbound tracer were separated by filtration through Whatman GF/C glass microfiber filters using a vacuum manifold, before γ-counting.

Calcium mobilization assay. FPR2-HEK 293 cells or freshly prepared PMNs were incubated with 2μM Fura 2-AM (Molecular Probes, Invitrogen) in Hanks balanced salt solution supplemented with 2mM $CaCl_2$ at 37°C for 1 hour in the dark. Subsequently, cells were washed and stimulants added at indicated concentrations. Ionomycin (1μM) was used as a positive control. Mobilization of intracellular calcium was measured by recording the ratio of fluorescence emission at 510 nm after sequential excitation at 340 and 380 nm using the NOVostar microplate reader (BMG Labtech).

Flow chamber assay. Human umbilical vein endothelial cells (HUVECs) were cultured until confluence and stimulated with 10 ng/mL tumor necrosis factor-α for 4 hours (Sigma-Aldrich). Isolated PMNs were incubated with AnxA1 or SAnxA1 for 10 minutes at 37°C, before flow over HUVEC monolayer at a rate of 1 dyn/cm^2, for 8 minutes, as described.[17] PMN/HUVEC interaction in the flow chamber was monitored on 6 random fields recorded for 10 seconds. Analysis of total cell capture, rolling, and firmly adherent PMNs was carried out off-line by manual quantification. In some cases, cells flowed over the HUVEC monolayers were collected and compared with resting (not-flowed) PMNs for the extent of membrane PR3 expression using a specific monoclonal antibody (ANCA anti-PR3, clone CLB12.8; Sanquin), and standard flow cytometric protocol.

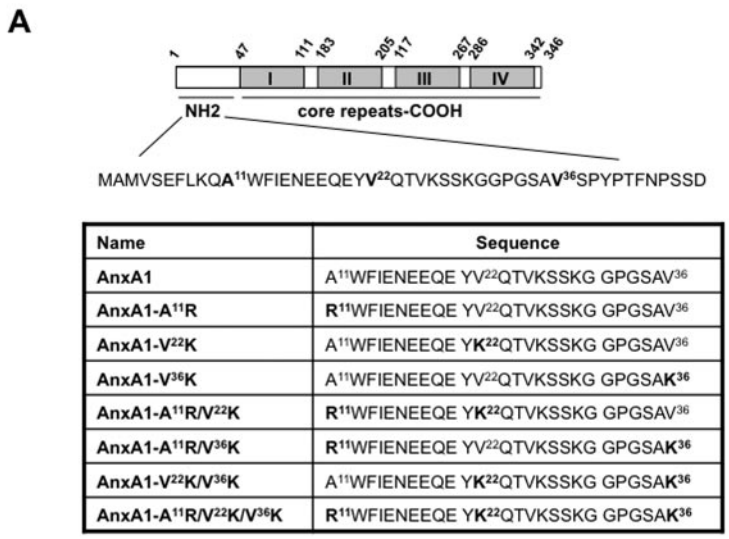

Name	Sequence
AnxA1	A[11]WFIENEEQE YV[22]QTVKSSKG GPGSAV[36]
AnxA1-A[11]R	**R[11]**WFIENEEQE YV[22]QTVKSSKG GPGSAV[36]
AnxA1-V[22]K	A[11]WFIENEEQE Y**K[22]**QTVKSSKG GPGSAV[36]
AnxA1-V[36]K	A[11]WFIENEEQE YV[22]QTVKSSKG GPGSA**K[36]**
AnxA1-A[11]R/V[22]K	**R[11]**WFIENEEQE Y**K[22]**QTVKSSKG GPGSAV[36]
AnxA1-A[11]R/V[36]K	**R[11]**WFIENEEQE YV[22]QTVKSSKG GPGSA**K[36]**
AnxA1-V[22]K/V[36]K	A[11]WFIENEEQE Y**K[22]**QTVKSSKG GPGSA**K[36]**
AnxA1-A[11]R/V[22]K/V[36]K	**R[11]**WFIENEEQE Y**K[22]**QTVKSSKG GPGSA**K[36]**

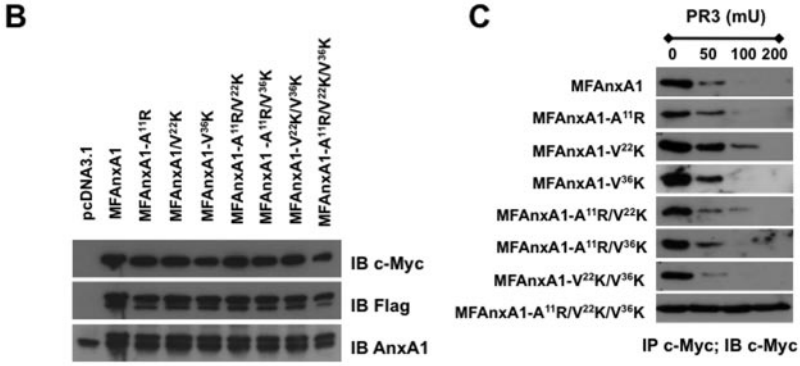

Figure 1. Effect of mutations in the N-terminal region of AnxA1 on cleavage by PR3. (A) Schematic representation of AnxA1 domains, highlighting the 3 PR3 cleavages sites in the N-terminal region; N-terminal domain sequences of AnxA1 and AnxA1 mutants. (B) Western blot analysis of MFAnxA1 mutants expression in HEK293 transfected cells: lysates were immunoblotted (IB) with anti–c-Myc, anti-Flag, and anti-AnxA1 antibodies. (C) Immunoprecipitation (IP) for c-Myc products were incubated for 30 minutes at 37°C with PR3 (50, 100, or 200 mU) and intact MFAnxA1 recovered by immunoblotting for c-Myc. Data are representative of 3 distinct analyses performed with distinct preparations of lysates.

Assessment of anti-inflammatory activity

Intravital microscopy of the mouse cremaster muscle. C57BL/6 or Fpr2 null mouse cremaster muscle microcirculation was prepared for intravital microscopy as described previously.[18] Briefly, mice were injected with 20 ng interleukin-1β (IL-1β; Peprotech) intrascrotally, and 2 hours after injection, anesthetized with a mixture of xylazine (7.5 mg/kg; Millpledge Pharmaceuticals) and ketamine (150 mg/kg; Amersham Biosciences). The right jugular vein was cannulated for drug administration. The testis was exposed through a small scrotal incision. The cremaster was mounted on a Zeiss Axioskop FS microscope and superfused with PBS at 37°C for a 30-minute stabilization period. A suitable postcapillary venule (wall shear rate $\geq$ 500 per second, 20 μm $<$ diameter $<$ 40 μm, length $\geq$ 100 μm) was selected and either vehicle (PBS-0.1% bovine serum albumin), AnxA1, or SAnxA1 (0.6 mg/kg, $\sim$ 400 pmol per mouse)[19] was injected via the jugular vein and microcirculation monitored for 30 minutes. Off-line analysis of leukocyte/endothelium interactions yielded the numbers for leukocytes flux (number of cells passing a fix point/minute) and cell adhesion (static cells for at least 30 seconds).

Skin edema. BALB/c mice (B&K Universal) were shaved from the mid-dorsal region and injected intradermally with 50 μL vehicle (Tyrode solution-0.1% bovine serum albumin) or N-formyl-Met-Leu-Phe (fMLF; 100 pmol) in the absence or presence of AnxA1 or SAnxA1 (1-100 ng). After 4 hours, mice were culled, and injection sites excised (5-mm biopsies). Samples were then processed for the myeloperoxidase (MPO) and PR3 activity.

Paw edema. C57BL/6 mice were lightly anesthetized and injected intraplantarly with 50 μL of 1% λ-carrageenan (Sigma-Aldrich). AnxA1 and SAnxA1 (1 μg) were administered together with λ-carrageenan. Edema, measured with a hydropletismometer (Ugo Basile), was calculated as previously described[20] by subtracting basal paw volumes.

MPO enzymatic activity. MPO activity was assessed by measuring the H_2O_2-dependent oxidation of 3,3′,5,5′-tetramethylbenzidine (0.05% wt/vol TMB-12.5% dimethyl sulfoxide) using skin and paw tissue samples, following a detailed protocol previously reported.[20] Assays were performed in triplicates and normalized for protein content.

Histology. Histologic analyses were conducted on paws collected 24 hours after λ-carrageenan. Fixed (4% formalin) samples were incubated with 0.1mM EDTA (ethylenediaminetetraacetic acid) for 14 days before paraffin embedding. Sections (5-μm) were deparaffinized and stained with hematoxylin and eosin. A minimum of $\geq$ 3 sections per animal were evaluated.

Statistical analysis

Data are expressed as mean plus or minus SEM. Student *t* test or analysis of variance were used for 2 or more groups. GraphPad Prism 4.0 software (GraphPad). In all cases, a *P* value $<$ .05 was taken as significant.

Results

Identification of SAnxA1

We began this study by determining the relative contribution of each PR3 sensitive site in the AnxA1 N terminus by generating a series of single, double, and triple mutants (Figure 1A). Site direct mutagenesis was carried out using as template a double-tagged AnxA1 (c-Myc on the N terminus and Flag at the C terminus; MFAnxA1)[11] allowing us to track down the clipped N terminus. Three single (A[11]R; V[22]K; V[36]K), 3 double (A[11]R/V[22]K; A[11]R/

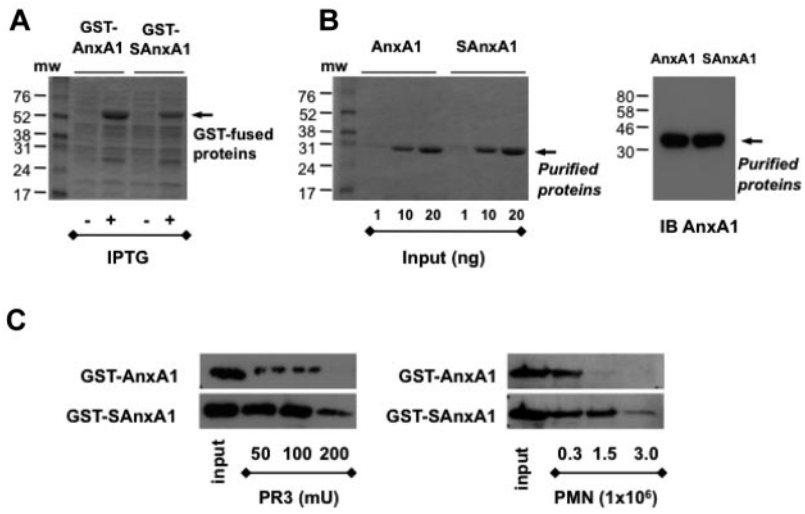

Figure 2. Purification of recombinant AnxA1 and SAnxA1 by chromatography. After cloning in the pGEX-6P-1 vector, in frame with GST, GST-tag was used to purify AnxA1 and SAnxA1 on a Glutathione Sepharose 4B column. (A) Coomassie blue-stained gel of recombinant GST-AnxA1 and GST-SAnxA1 expressed in BL21 cells after IPTG treatment. (B) Coomassie blue-stained gel of recombinant AnxA1 and SAnxA1 recovered after GST tag removal, using PreScission Protease. Immunoblot (IB) of purified recombinant AnxA1 and SAnxA1, using a specific anti-AnxA1 antibody. (C) Western blotting analysis of AnxA1 and SAnxA1 cleavage by recombinant PR3 and PMN lysates, after incubation for 30 minutes at 37°C. Results are representative of 3 distinct preparations and experiments.

$V^{36}K$; $V^{22}K/V^{36}K$), and one triple ($A^{11}R/V^{22}K/V^{36}K$) MFAnxA1 mutants were cloned and produced by transfection in HEK293 cells (Figure 1B). For the in vitro AnxA1 cleavage assay, cell lysates were immunoprecipitated with anti–c-Myc and then incubated with increasing amount of recombinant PR3 for 30 minutes at 37°C. As shown in Figure 1C, none of the single mutants presented any significant difference in their cleavage by PR3, compared with the parental protein MFAnxA1, the exception being mutant $V^{22}K$, which was modestly resistant to 100 mU PR3. Consistent with this, the double-mutant $A^{11}R/V^{22}K$ demonstrated similar partial resistance to cleavage by PR3, with no further improvement being added by the second mutation on $A^{11}R$ (Figure 1C). This systematic analysis showed that the triple mutant $A^{11}R/V^{22}K/V^{36}K$ displayed complete resistance to PR3 cleavage at all the concentrations tested. Based on these results, further characterization of the triple mutant, christened super AnxA1 or SAnxA1, was then performed.

Purification of recombinant AnxA1 and SAnxA1

Untagged AnxA1 and SAnxA1 were subcloned in pGEX-6P1 GST vector to transform *E coli* BL21 cells, and both proteins could be recovered from the cell lysates (Figure 2A). Highly purified proteins were obtained using GST-purification and in-column tag removal system as assessed by Blue Coomassie staining and immunoblot for AnxA1 (Figure 2B). When the cleavage assay was run with PR3, SAnxA1 was confirmed to be more resistant than parent AnxA1 (Figure 2C). Of importance, the same held true when PMN extracts were used as cleaving material: SAnxA1 was approximately 5 times more resistant than AnxA1.

SAnxA1 retains AnxA1 bioactivity at FPR2

Next, we investigated whether the mutations inserted in SAnxA1 would influence its biologic activity in vitro. In the binding assay to FPR2-HEK293 cells, incubation with AnxA1 competed with the tracer with an apparent half maximal inhibitory concentration of 150 ± 5nM (comparable with our previous data[17]); SAnxA1 retained specific binding with a half maximal inhibitory concentration of 590nM (~ 4-fold lower affinity than AnxA1; Figure 3A). This slight reduced binding affinity to FPR2 was not reflected in SAnxA1 ability to activate FPR2 as tested by Erk phosphorylation (Figure 3B) or Ca^{2+} fluxes (Figure 3C) in FPR2-HEK293. The latter readout allowed us to test SAnxA1 on isolated PMNs: stimulation of these cells with 1 nM SAnxA1 elicited a sustained increase in $[Ca^{2+}]_i$ (peak value ~ 1.4) comparable with the response obtained with AnxA1 (peak value ~ 1.3). We next compared the $[Ca^{2+}]_i$ maximal values obtained, using different concentrations of AnxA1 and SAnxA1 (0.1 or 1nM) and ionomycin as a positive control: in line with the data with FPR2-HEK (Figure 3C), no significant differences in PMNs downstream signal was measured (Figure 3D). Next we tested whether these effects would lead to modulation of PMN reactivity.

SAnxA1 blocks PMN interaction with endothelial cells: indication for higher efficacy

In the flow chamber assay, SAnxA1 (10nM) produced profound inhibition on PMN interaction with HUVEC monolayers: see representative images in Figure 4A. Detailed analyses revealed that both AnxA1 and SAnxA1 affected PMN capture, rolling, and adhesion, but the latter readout was significantly more inhibited by SAnxA1 (Figure 4B). Such an effect was concentration-dependent and optimal at 10nM for either recombinant protein (Figure 4C). Noteworthy, this protocol leads to partial PMN activation as evident from cell surface PR3 expression which almost doubles in PMNs flowed over the HUVEC monolayer; values of median fluorescence intensity of 81 ± 2.5 and 143 ± 8.3 for unstimulated and flowed PMNs, respectively, could be calculated in 4 distinct cell preparations and experiments ($P < .05$).

To determine the impact of SAxnA1 (and AnxA1) on leukocyte/endothelium interaction in vivo, the mouse cremasteric microcirculation inflamed with IL-1β was used.[21] Injection of the cytokine provoked a marked inflammation with changes in both the extent of cell flux (Figure 5A), rolling cell velocity (31 ± 10 and 3.1 ± 0.1 μm/s, for vehicle and IL-1β, respectively) and cell adhesion (Figure 5A). Injection of either AnxA1 or SAnxA1 modified the on-going inflammation in a different way. Both AnxA1 and SAnxA1 augmented cell velocity, with a significant effect at ≥ 10 minutes after treatment (Figure 5B), an effect mirrored by the reduced degree of cell adhesion (Figure 5C). Importantly, the effect of SAnxA1 incremented over time (eg, see cell adhesion at 30 minutes after administration; ~ 50% inhibition) whereas that of the natural protein peaked at the 20 minutes time point (~ 30% inhibition of cell adhesion; Figure 5C). Importantly, either recombinant protein was ineffective in animals nullified for the murine formyl-peptide receptor 2 (the ortholog of human FPR2; Figure 5D shows the data for cell adhesion).

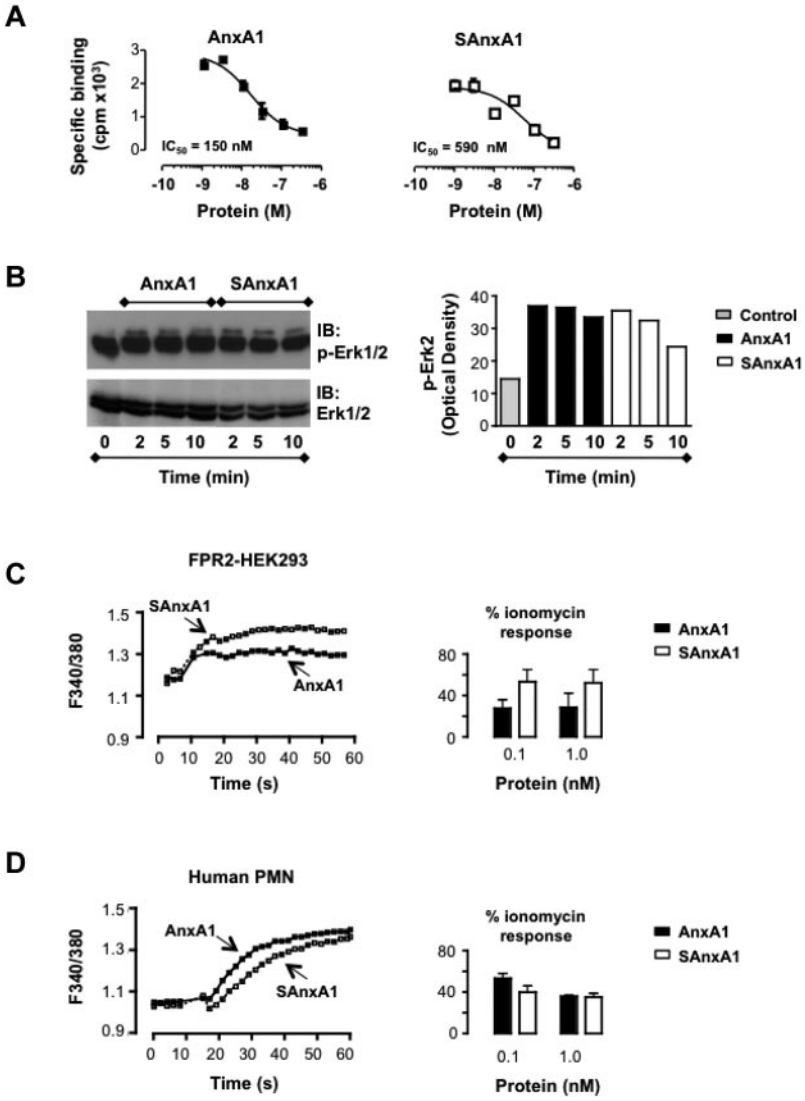

Figure 3. SAnxA1 binds and activates human FPR2. (A) Analysis of competition binding in FPR2-HEK293 cells using AnxA1 and SAnxA1 to compete with the tracer (W peptide; 82pM). Representative of 2 experiments in triplicate. (B) FPR2-HEK293 cells were incubated with 1nM AnxA1 and SAnxA1, for the indicated times, to determine the level of Erk1/2 phosphorylation by Western blot using anti–p-Erk1/2 antibody. The bar graph reports the densitometric analysis of the p-Erk2 bands shown on the left. Representative of 3 experiments. Calcium mobilization in (C) FPR2-HEK293 cells and (D) isolated PMNs. In all cases, cells were loaded with 2μM Fura-2 and analyzed for $[Ca^{2+}]i$ changes after 0.1-1nM AnxA1 or SAnxA1. Fluorescence ratios tracing of representative experiment recorded in a dual excitation fluorescent spectrophotometer are shown (left panels). Maximal intracellular calcium increased induced by different concentration of AnxA1 or SAnxA1 (0.1 or 1nM) were normalized to the response induced by ionomycin (1μM; taken as 100%; right panels). Values are expressed as the mean ± SEM of 3 independent experiments.

SAnxA1 shows increased and prolonged anti-inflammatory activity

Next, we established if SAnxA1 and AnxA1 displayed anti-inflammatory activities with a different profile, applying in more complex models of inflammation, where PMN activation and recruitment is the end point of multiple processes. Intradermal injection of fMLF provoked marked PMN accumulation that could be reliably quantified by MPO activity: 180 ± 30 and 350 ± 44 mU MPO/mg tissue for vehicle- and fMLF-treated skin sites, respectively. Coadministration of AnxA1 or SAnxA1 (1-100 ng equivalent to 0.24-24 pmol/site) inhibited the cellular response to fMLF, with the mutant protein affording significantly higher degree of inhibition (Figure 6A).

To study SAnxA1 biologic properties over a longer time-frame, the mouse paw edema model was used.[20] Intra-paw injection of λ-carrageenan provokes a marked localized inflammatory response that peaks early on (2 hours) as well as at later time points (24 hours after injection; Figure 6B). Coinjection of AnxA1 or SAnxA1 induced a mild but yet significant inhibition of paw edema (47% and 30%, respectively) at 4 hours. Conversely, as the edema progressed to the second peak, only the SAnxA1 displayed significant inhibitory properties (~ 30%; Figure 6B). These macroscopic measurements were corroborated by histologic analyses, whereby reduced infiltration of inflammatory leukocytes could be seen in both AnxA1- and SAnxA1-treated paw section (4-hour time point; Figure 6C) whereas low numbers of cells at 24 hours after λ-carrageenan could be observed only in the SAnxA1 group (Figure 6C). Finally, biochemical determination of MPO activity in 24 hours paw extracts revealed 5500 ± 200 versus 2200 ± 100 mU/mg tissue, for vehicle- and SAnxA1-treated paws, respectively ($P < .001$, 6 mice per group).

Discussion

In this study we report generation and characterization of an AnxA1 mutant able to resist to PR3 (and other proteases present on PMN extracts) cleavage. SAnxA1 displays exquisite anti-PMN properties both in vitro and in vivo, with particular efficacy on PMN interaction with inflamed endothelia. These data demonstrate that AnxA1 cleavage (at least the one effected by serine proteases) is not a prerequisite for biologic efficacy but rather a catabolic event, as originally hypothesized.[4,11]

One of the hallmarks of PMN activation is release of proteinases such as cathepsin G, elastase, and PR3.[22] These potent biologic weapons help neutrophils to transmigrate across the endothelial

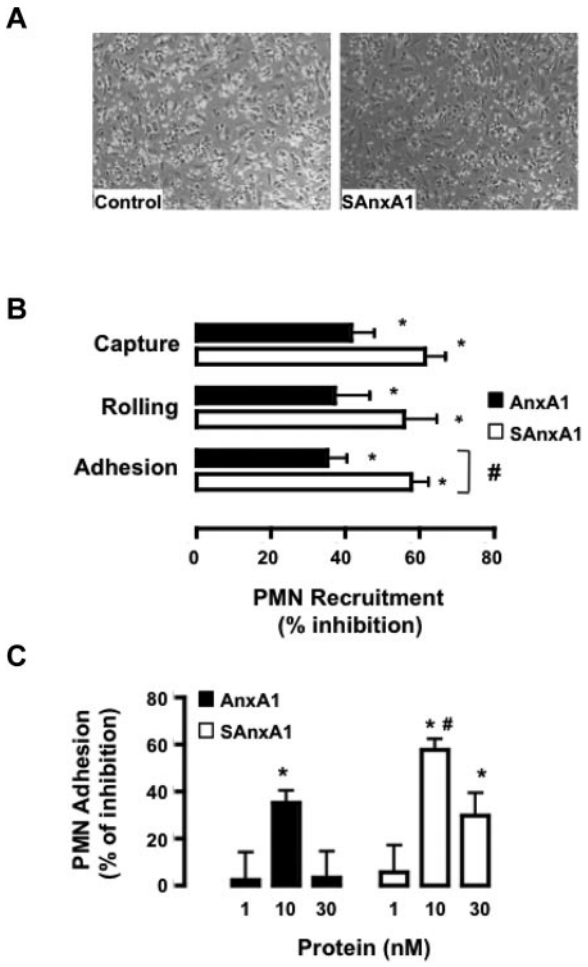

Figure 4. SAnxA1 inhibits PMN interaction with HUVECs. (A) Representative images of the flow chamber assay. Isolated PMNs were incubated with 10nM SAnxA1 for 10 minutes before flow over tumor necrosis factor-stimulated HUVEC monolayers. (B) Cumulative data for PMN capture, rolling, and adhesion after incubation with 10nM AnxA1 or SAnxA1 and flow over the HUVECs. (C) Concentration response for AnxA1 and SAnxA1 on the extent of PMN adhesion to HUVECs under flow. Data are mean ± SEM of 3 experiments performed with distinct donor cells. $*P < .01$ versus vehicle (as calculated on original values) and $\#P < .05$ versus respective AnxA1 dataset.

wall[23] as well as to fight pathogens,[24] facilitating disposal of potentially harmful products released during inflammation and infections.[25,26] However, current view on the role of these proteinases in PMN biology suggest more than protein-degrading enzymes so that they can affect several pathophysiologic signaling pathways.[27] For instance, studies have shown that release of PR3 and human neutrophil elastase (HNE) from activated PMNs can result in their entry into endothelial cells where they can directly cleave p65 subunit of nuclear factor-κB in the N- and C-terminal region, respectively,[28] affecting cytokine synthesis.[25,29]

Our interest on these enzymes stems from the observation that cleaved AnxA1 is released/detected in the supernatant of activated PMNs[5] as well as in neutrophilic inflammatory exudates.[14,15] Restricting our attention to the microenvironment of an activated PMNs, we found a pivotal role for PR3 in cleaving endogenous AnxA1,[11] thus providing another example of contribution of these proteinases to the modulation of signaling pathways. Matrix-assisted laser desorption/ionization time-of-flight analysis of the peptides originated from AnxA1 treatment with PR3 or PMN membrane fractions allowed us to single out 3 potential cleavage recognition sites located at A^{11}, V^{22}, and V^{36} (see 11). In our experimental settings, PR3 cleavage of AnxA1 N terminus can occur at all 3 sites; congruently, SAnxA1 was highly resistant to proteolysis by recombinant PR3 and PMN extracts.

The identification of an uncleavable form of AnxA1 allow us to address a fundamental question in the biology of AnxA1, and possibly other Annexins[10,30]: whether cleavage of the N terminus is an activating process leading to the release of the bioactive core of the protein or a catabolic event terminating its action. In resting PMNs, AnxA1 resides in the gelatinase granules and is rapidly exported on the cells surface upon cell stimulation,[31] to modulate the extent of PMN adhesion and emigration, often promoting cell detachment.[7,17,19] Once at the site of inflammation, de novo AnxA1 synthesis occurs, likely to modulate PMN apoptosis and phagocytosis by resident macrophages as well as instruct T cells toward activation and expansion (for review see[4,32]). Most of these effects of AnxA1 are conveyed by specific receptors, namely FPR2,[33] as demonstrated for antiadhesive[7] and apoptotic[9] actions, though intriguingly, a recent study indicated the central core of AnxA1 (amino acids 47-346) as responsible for the recognition of apoptotic Jurkat cells by phagocytes,[34] suggesting different biologic functions between the N terminus and the main core of this protein.

Once SAnxA1 was generated and validated, it was important to test that the mutations had not modified fundamental structural and functional characteristics of the protein. Binding to FPR2 was tested and retained, although with an apparent reduction in affinity. It should be noted that, in line with what argued for the native protein,[17] use of short peptides as tracers (because AnxA1 cannot be radioiodinated without loss of activity) may lead to underestimate its affinity to this receptor. Indeed, the same apparent discrepancy was reported in our previous study with recombinant AnxA1.[17] In these experiments, both AnxA1 and SAnxA1 were able to activate FPR2-downstream responses at concentrations much lower (0.1-1nM) than those required to displace radiolabeled W peptide.

In a separate study, the effects of 6 FPR peptides were tested on actin polymerization and oxidant production in human PMNs; although all ligands showed similar efficacy for both responses,[35] their potencies/affinities varied over 3 and 4 orders of magnitude for actin polymerization and oxidant production, respectively. Such an effect has been explained in terms of selective stabilization of different active receptor states and by the fact that the kinetic lifetimes of particular ligand-receptor complexes play an important role in determining signaling outcomes. In other words, different ligands may produce not only different numbers but also different lifetimes of receptor states relevant to production of a given response.

Whereas there was no major difference between AnxA1 and SAnxA1 in eliciting postreceptor events, some degree of distinctions emerged when PMN reactivity on inflamed endothelia was analyzed. Indeed, it is highly likely (and in part we could demonstrate it in the flow assay) that PR3 can be rapidly activated on the PMN cell surface in these experimental conditions.[36,37] Preincubated with isolated PMNs, SAnxA1 could produce significant inhibition of their reactivity with the HUVEC monolayer, with higher efficacy than the parent protein on the extent of PMN adhesion. Such an effect is highly likely to occur via FPR2,[17] however we cannot exclude that mutations in SAnxA1 might have not altered ability to bind other members of this receptor family, in line with data generated with N-terminal–derived peptides.[38,39] Indeed, SAnxA1 affected PMN rolling by $> 50\%$, an effect displayed by short N-terminal peptides and proposed to stem from FPR1 activation.[17] Irrespective of the molecular target, these

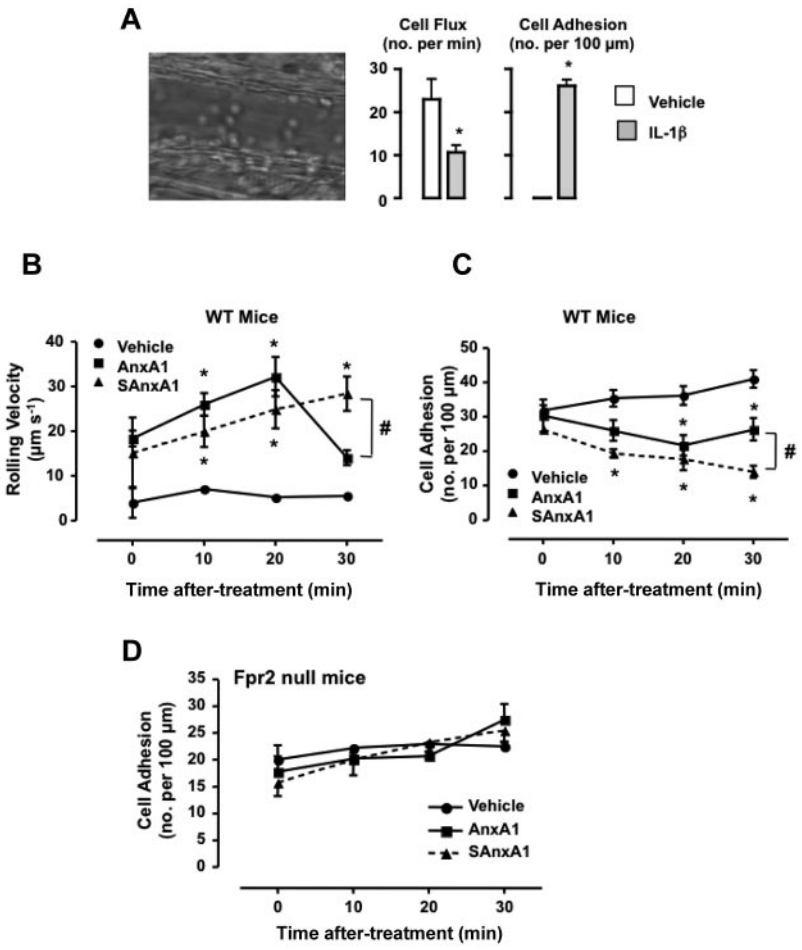

Figure 5. Longer lasting effect of SAnxA1 on leukocyte adhesion in postcapillary venules. Mice were injected intrascrotally with either saline or 50 ng IL-1β, and the extent of leukocyte rolling and adhesion was quantified 3 hours later. Image is representative of the inflammatory status induced by the cytokine. Data are mean ± SEM of 6 mice per group. *$P < .01$ versus vehicle. Mice pretreated with IL-1β were instrumented an administered via the jugular vein with PBS, AnxA1 (0.6 mg/kg), or SAnxA1 (0.6 mg/kg), and the microcirculation monitored for further 30 minutes both for cell rolling velocity (B) and cell adhesion (C). Values are mean ± SEM of 5 mice per group. *$P < .01$ versus vehicle group and #$P < .05$ versus respective AnxA1 group. (D) FPR2 null mice were treated with IL-1β and recombinant proteins as described in panels B-C. Values are mean ± SEM of 5 mice per group.

molecular and functional experiments encouraged us to test SAnxA1 in more stringent experimental settings. To this end, analysis of the inflamed microvasculature was conducted. In fact, previous studies revealed potent inhibitory properties of AnxA1 and peptides derived from the N-terminal region[19] with antiadhesive properties likely to occur via activation of the FPR2 ortholog.[7,40] Moreover, cell recruitment to the postcapillary venule endothelium is under tonic inhibitory control of endogenous AnxA1.[18] After inflammation of the microcirculation with IL-1β, reduction in the extent of cell flux (associated with proper rolling phenomenon, ie, low cell velocity on the endothelium) was complemented with increased in cell adhesion. Whereas an anti-inflammatory dose of AnxA1[19] did not affect IL-1β–induced modifications in cell rolling, SAnxA1 brought this process back to the values measured in vehicle-treated mice. Another striking difference was seen with respect to cell adhesion again with SAnxA1 displaying prolonged inhibitory properties. We could not determine the activation/involvement of PR3 (and other serine proteases, for that matter) in these microvascular events but in analogy to the flow chamber study with isolated PMNs, we hypothesize that leukocyte rolling and adhesion is a sufficient stimulus to activate PR3. Indeed, serine proteases have a function on the process of cell adhesion and emigration, with most studies addressing the potential of elastase,[26,29,41] because of their expression on the cell surface of the adherent and migrating leukocyte.[42] Using the recently described Fpr2 null mouse colony,[40] we could demonstrate that the inhibitory effects of SAnxA1, and indeed AnxA1, relied entirely on this specific receptor.

In any case, these results suggest that reducing AnxA1 cleavage greatly influences the ability of this homeostatic mediator to affect PMN adhesion to inflamed endothelial cells. This amelioration is reflected by SAnxA1 potency and, more importantly, time-dependency compared with naive AnxA1, highlighting a unique aspect of the anti-inflammatory properties of AnxA1. We propose a model whereby a counter-regulatory function of AnxA1 on PMN adhesion is modulated by the coordinated action of PR3: all this would satisfy a homeostatic function to regulate the extent of PMN trafficking in acute vascular inflammation.

In final part of the study, we determined the anti-inflammatory potential of SAnxA1 in the context of more severe inflammatory settings. In the fMLF-induced skin model, extravasated PMNs remain trapped at the inflammatory site creating a localized pool of serine proteases and other enzymes. It was reassuring to observe that as low as 27 fmol SAnxA1 delivered locally to the site of inflammatory insult provoked marked (> 60%) attenuation of the MPO activity detected, with a doubling/trebling efficacy over natural AnxA1. Another predicted characteristic of SAnxA1 would be a longer lasting effect, a hint for which emerged in the experiments of intravital microscopy. To expand on this hypothesis, we tested the properties of the 2 recombinant proteins in the mouse paw edema model[20] characterized by an early phase and a delayed phase of inflammation. We chose the local route of administration to increase the exposure of the proteins to PR3 and other proteolytic enzymes carried to the site of inflammation by the migrating PMNs. Whereas both AnxA1 and SAnxA1 inhibited, with no apparent difference, the early response at time 4 hours, only

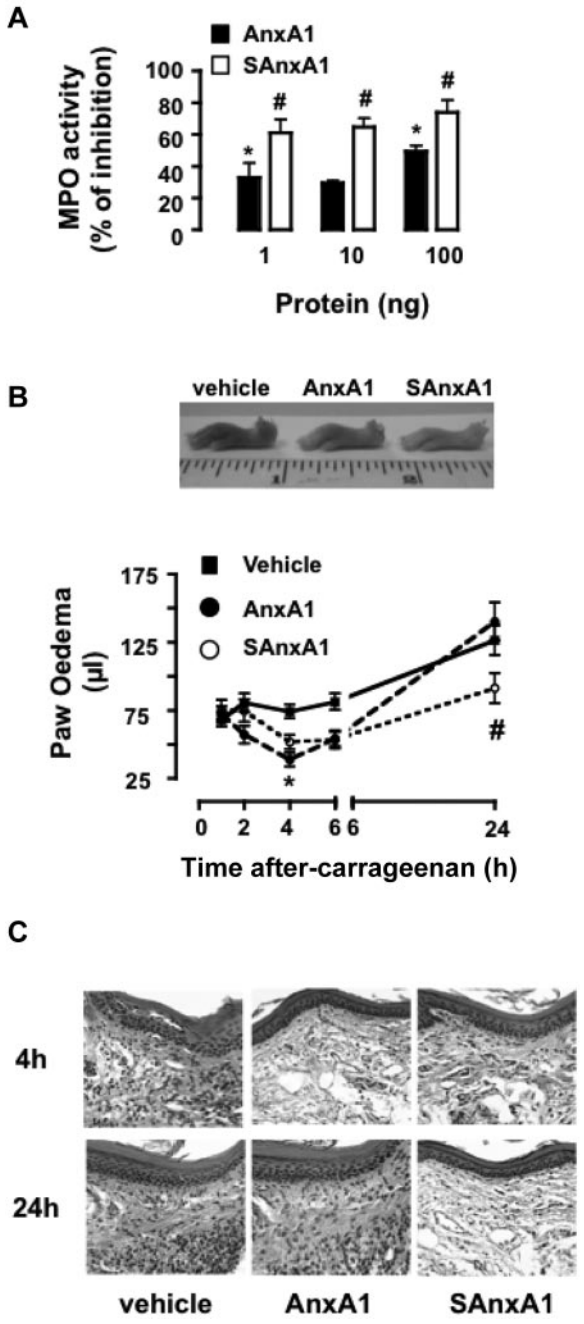

Figure 6. SAnxA1 displays longer-lasting inhibitory effects on PMN recruitment and inflammation in vivo. (A) Mice were treated intradermally with fMLF (100 pmol) and the reported doses of AnxA1 and SAnxA1. Four hours later, skin samples (5-mm biopsies) were harvested and assayed for MPO activity. MPO activity values in fMLF-treated skin sites were 350 ± 44 mU/mg of tissue (taken as 100% control). Data are mean ± SEM of 4 separate experiments with 3-7 mice/group. (B) Time course of λ-carrageenan-induced paw edema in mice locally treated with PBS (50 µL), AnxA1 (1 µg), or SAnxA1 (1 µg). Values are mean ± SEM of 3 separate experiments with n = 6 mice per group. Representative images of the paw collected 24 hours after treatment. *$P < .05$ vs. vehicle group and #$P < .05$ versus respective AnxA1 group. (C) Hematoxylin and eosin staining of paw tissue samples collected 4 and 24 hours after λ-carrageenan in mice treated with either vehicle, AnxA1, or SAnxA1 as in panel B. Images are representative of analyses of tissue samples from 4 mice.

SAnxA1 was effective on the marked inflammation measured 24-hours after λ-carrageenan. These results do not allow us to dissect the mechanism(s) behind this long lasting effect, apart from proposing resistance to cleavage hence longer presence at the inflammatory site. We cannot exclude the involvement of other pathways in the striking effect of SAnxA1, persisting within the inflamed paw, on the 24-hour edema, including promotion of retrograde leukocyte transmigration[43,44] and/or removal of apoptotic leukocytes.[9] In any case, we observed major reductions in immune cell infiltrates in the 24-hours after λ-carrageenan. Tissue samples of mice treated with SAnxA1 was observed by histology and quantified by MPO activity.

We believe the novel findings here presented open up 2 important considerations. First, that pathologic conditions characterized by increased membrane expression of PR3 could lead to potential harmful effects because of a misbalanced action of this catabolic enzyme on the homeostatic action of the endogenous AnxA1 pathway. Such an example could be the Wegener granulomatosis: a form of small-vessel vasculitis characterized by primed PMNs flowing in the bloodstream.[45] Second, agents targeting directly or indirectly the PR3/AnxA1 pathway could be a valid novel therapeutic strategy to disentangle trapped PMNs from inflamed microvasculature in these diseases. Consistent with this, it is important to note that glucocorticoids, potent anti-inflammatory drugs used in different types of vasculitis including Wegener granulomatosis, positively modulate AnxA1 expression and release in PMNs[46] and can also up-regulate the receptors for this mediator.[47-49] We propose treatment of small (and possibly large) vessel vasculitides with glucocorticoids would increase the rate of expression and/or release of AnxA1, thus counteracting the increased catabolism that would be occurring on the PMN cell surface.

In conclusion, we have unveiled a novel piece in the complex puzzle of the PMN AnxA1 biologic system. These findings may be beneficial for the design of inhibitors aimed at neutralizing the cleavage activity of PR3 toward endogenous AnxA1, representing a possible avenue for novel therapeutic discovery programs.

Acknowledgments

The authors thank C. de Chiara (Division of Molecular Structure, National Institute for Medical Research, London, United Kingdom) for her help and expertise in protein purification and V. Brancaleone and S. Bena (William Harvey Research Institute, Barts and The London School of Medicine, London, United Kingdom) for their technical assistance in obtaining the Calcium flux data.

This work was funded by the British Heart Foundation (PG/06/153/22 042). This work forms part of the research themes contributing to the translational research portfolio of Barts and the London Cardiovascular Biomedical Research Unit, which is supported and funded by the National Institutes of Health Research.

Authorship

Contribution: M.P.-R. performed experiments, analyzed data, and wrote the first draft of the manuscript; F.M., D.C., A.A.-K., and J.D. performed experiments and analyzed data; M.P. planned the project and wrote the manuscript; and F.D.A. planned the project, analyzed data, and wrote the manuscript.

Conflict-of-interest disclosure: The authors declare no competing financial interests.

Correspondence: Fulvio D'Acquisto, The William Harvey Research Institute, Center for Biochemical Pharmacology, Charterhouse Square, London EC1M 6BQ, United Kingdom; e-mail: f.dacquisto@qmul.ac.uk.

References

1. Nathan C. Neutrophils and immunity: challenges and opportunities. *Nat Rev Immunol.* 2006;6(3):173-182.
2. Serhan CN, Brain SD, Buckley CD, et al. Resolution of inflammation: state of the art, definitions and terms. *FASEB J.* 2007;21(2):325-332.
3. Serhan CN, Chiang N, Van Dyke TE. Resolving inflammation: dual anti-inflammatory and pro-resolution lipid mediators. *Nat Rev Immunol.* 2008;8(5):349-361.
4. Perretti M, D'Acquisto F. Annexin A1 and glucocorticoids as effectors of the resolution of inflammation. *Nat Rev Immunol.* 2009;9(1):62-70.
5. Perretti M, Croxtall JD, Wheller SK, Goulding NJ, Hannon R, Flower RJ. Mobilizing lipocortin 1 in adherent human leukocytes downregulates their transmigration. *Nat Med.* 1996;2(11):1259-1262.
6. Perretti M, Chiang N, La M, et al. Endogenous lipid- and peptide-derived anti-inflammatory pathways generated with glucocorticoid and aspirin treatment activate the lipoxin A4 receptor. *Nat Med.* 2002;8(11):1296-1302.
7. Gavins FN, Yona S, Kamal AM, Flower RJ, Perretti M. Leukocyte antiadhesive actions of annexin 1: ALXR- and FPR-related anti-inflammatory mechanisms. *Blood.* 2003;101(10):4140-4147.
8. Strausbaugh HJ, Rosen SD. A potential role for annexin 1 as a physiologic mediator of glucocorticoid-induced L-selectin shedding from myeloid cells. *J Immunol.* 2001;166(10):6294-6300.
9. Scannell M, Flanagan MB, deStefani A, et al. Annexin-1 and peptide derivatives are released by apoptotic cells and stimulate phagocytosis of apoptotic neutrophils by macrophages. *J Immunol.* 2007;178(7):4595-4605.
10. Gerke V, Moss SE. Annexins: from structure to function. *Physiol Rev.* 2002;82(2):331-371.
11. Vong L, D'Acquisto F, Pederzoli-Ribeil M, et al. Annexin 1 cleavage in activated neutrophils: a pivotal role for proteinase 3. *J Biol Chem.* 2007;282(41):29998-30004.
12. Perretti M, Flower RJ. Modulation of IL-1-induced neutrophil migration by dexamethasone and lipocortin 1. *J Immunol.* 1993;150(3):992-999.
13. Gavins FN, Dalli J, Flower RJ, Granger DN, Perretti M. Activation of the annexin 1 counter-regulatory circuit affords protection in the mouse brain microcirculation. *Faseb J.* 2007;21(8):1751-1758.
14. Vergnolle N, Coméra C, Buéno L. Annexin 1 is overexpressed and specifically secreted during experimentally induced colitis in rats. *Eur J Biochem.* 1995;232:603-610.
15. Tsao FH, Meyer KC, Chen X, Rosenthal NS, Hu J. Degradation of annexin I in bronchoalveolar lavage fluid from patients with cystic fibrosis. *Am J Respir Cell Mol Biol.* 1998;18(1):120-128.
16. Sugawara S. Immune functions of proteinase 3. *Crit Rev Immunol.* 2005;25(5):343-360.
17. Hayhoe RP, Kamal AM, Solito E, Flower RJ, Cooper D, Perretti M. Annexin 1 and its bioactive peptide inhibit neutrophil-endothelium interactions under flow: indication of distinct receptor involvement. *Blood.* 2006;107(5):2123-2130.
18. Chatterjee BE, Yona S, Rosignoli G, et al. Annexin 1-deficient neutrophils exhibit enhanced transmigration in vivo and increased responsiveness in vitro. *J Leukoc Biol.* 2005;78(3):639-646.
19. Lim LH, Solito E, Russo-Marie F, Flower RJ, Perretti M. Promoting detachment of neutrophils adherent to murine postcapillary venules to control inflammation: effect of lipocortin 1. *Proc Natl Acad Sci U S A.* 1998;95(24):14535-14539.
20. Maione F, Paschalidis N, Mascolo N, Dufton N, Perretti M, D'Acquisto F. Interleukin 17 sustains rather than induces inflammation. *Biochem Pharmacol.* 2009;77(5):878-887.
21. Dangerfield JP, Wang S, Nourshargh S. Blockade of alpha6 integrin inhibits IL-1beta- but not TNF-alpha-induced neutrophil transmigration in vivo. *J Leukoc Biol.* 2005;77(2):159-165.
22. Sengeløv H, Kjeldsen L, Borregaard N. Control of exocytosis in early neutrophil activation. *J Immunol.* 1993;150(4):1535-1543.
23. Owen CA, Campbell EJ. The cell biology of leukocyte-mediated proteolysis. *J Leukoc Biol.* 1999;65(2):137-150.
24. Levy O. Antibiotic proteins of polymorphonuclear leukocytes. *Eur J Haematol.* 1996;56(5):263-277.
25. Adkison AM, Raptis SZ, Kelley DG, Pham CT. Dipeptidyl peptidase I activates neutrophil-derived serine proteases and regulates the development of acute experimental arthritis. *J Clin Invest.* 2002;109(3):363-371.
26. Raptis SZ, Shapiro SD, Simmons PM, Cheng AM, Pham CT. Serine protease cathepsin G regulates adhesion-dependent neutrophil effector functions by modulating integrin clustering. *Immunity.* 2005;22(6):679-691.
27. Meyer-Hoffert U. Neutrophil-derived serine proteases modulate innate immune responses. *Front Biosci.* 2009;14:3409-3418.
28. Preston GA, Zarella CS, Pendergraft WF III, et al. Novel effects of neutrophil-derived proteinase 3 and elastase on the vascular endothelium involve in vivo cleavage of NF-kappaB and proapoptotic changes in JNK, ERK, and p38 MAPK signaling pathways. *J Am Soc Nephrol.* 2002;13(12):2840-2849.
29. Young RE, Thompson RD, Larbi KY, et al. Neutrophil elastase (NE)-deficient mice demonstrate a nonredundant role for NE in neutrophil migration, generation of proinflammatory mediators, and phagocytosis in response to zymosan particles in vivo. *J Immunol.* 2004;172(7):4493-4502.
30. Rescher U, Gerke V. Annexins—unique membrane binding proteins with diverse functions. *J Cell Sci.* 2004;117(Pt 13):2631-2639.
31. Perretti M, Christian H, Wheller SK, et al. Annexin I is stored within gelatinase granules of human neutrophil and mobilized on the cell surface upon adhesion but not phagocytosis. *Cell Biol Int.* 2000;24(3):163-174.
32. D'Acquisto F. On the adaptive nature of annexin-A1. *Curr Opin Pharmacol.* 2009;9(4):521-528.
33. Ye RD, Boulay F, Wang JM, et al. International Union of Basic and Clinical Pharmacology. LXXIII. Nomenclature for the formyl peptide receptor (FPR) family. *Pharmacol Rev.* 2009;61(2):119-161.
34. Blume KE, Soeroes S, Waibel M, et al. Cell surface externalization of annexin A1 as a failsafe mechanism preventing inflammatory responses during secondary necrosis. *J Immunol.* 2009;183(12):8138-8147.
35. Waller A, Sutton KL, Kinzer-Ursem TL, et al. Receptor binding kinetics and cellular responses of six N-formyl peptide agonists in human neutrophils. *Biochemistry.* 2004;43(25):8204-8216.
36. Witko-Sarsat V, Rieu P, Descamps-Latscha B, Lesavre P, Halbwachs-Mecarelli L. Neutrophils: molecules, functions and pathophysiological aspects. *Lab Invest.* 2000;80(5):617-653.
37. Pederzoli M, Kantari C, Gausson V, Moriceau S, Witko-Sarsat V. Proteinase-3 induces procaspase-3 activation in the absence of apoptosis: potential role of this compartmentalized activation of membrane-associated procaspase-3 in neutrophils. *J Immunol.* 2005;174(10):6381-6390.
38. Ernst S, Lange C, Wilbers A, Goebeler V, Gerke V, Rescher U. An annexin 1 N-terminal peptide activates leukocytes by triggering different members of the formyl peptide receptor family. *J Immunol.* 2004;172(12):7669-7676.
39. Walther A, Riehemann K, Gerke V. A novel ligand of the formyl peptide receptor: annexin I regulates neutrophil extravasation by interacting with the FPR. *Mol Cell.* 2000;5(5):831-840.
40. Dufton N, Hannon R, Brancaleone V, et al. The anti-inflammatory role of the murine formyl peptide receptor Fpr2: ligand-specific effects on leukocyte responses and experimental inflammation. *J Immunol.* 2010;184(5):2611-2619.
41. Nourshargh S, Marelli-Berg FM. Transmigration through venular walls: a key regulator of leukocyte phenotype and function. *Trends Immunol.* 2005;26(3):157-165.
42. Cepinskas G, Sandig M, Kvietys PR. PAF-induced elastase-dependent neutrophil transendothelial migration is associated with the mobilization of elastase to the neutrophil surface and localization to the migrating front. *J Cell Sci.* 1999;112(Pt 12):1937-1945.
43. Buckley CD, Ross EA, McGettrick HM, et al. Identification of a phenotypically and functionally distinct population of long-lived neutrophils in a model of reverse endothelial migration. *J Leukoc Biol.* 2006;79(2):303-311.
44. Lee JY, Buzney CD, Poznansky MC, Sackstein R. Dynamic alterations in chemokine gradients induce transendothelial shuttling of human T cells under physiologic shear conditions. *J Leukoc Biol.* 2009;86(6):1285-1294.
45. Kallenberg CG. Antineutrophil cytoplasmic autoantibody-associated small-vessel vasculitis. *Curr Opin Rheumatol.* 2007;19(1):17-24.
46. Goulding NJ, Godolphin JL, Sharland PR, et al. Anti-inflammatory lipocortin 1 production by peripheral blood leucocytes in response to hydrocortisone. *Lancet.* 1990;335(8703):1416-1418.
47. Sawmynaden P, Perretti M. Glucocorticoid up-regulation of the annexin-A1 receptor in leukocytes. *Biochem Biophys Res Commun.* 2006;349(4):1351-1355.
48. Ehrchen J, Steinmuller L, Barczyk K, et al. Glucocorticoids induce differentiation of a specifically activated, anti-inflammatory subtype of human monocytes. *Blood.* 2007;109(3):1265-1274.
49. Hashimoto A, Murakami Y, Kitasato H, Hayashi I, Endo H. Glucocorticoids co-interact with lipoxin A4 via lipoxin A4 receptor (ALX) up-regulation. *Biomed Pharmacother.* 2007;61(1):81-85.

2010 116: 4288-4296
doi:10.1182/blood-2010-02-270520 originally published online August 12, 2010

Design and characterization of a cleavage-resistant Annexin A1 mutant to control inflammation in the microvasculature

Magali Pederzoli-Ribeil, Francesco Maione, Dianne Cooper, Adam Al-Kashi, Jesmond Dalli, Mauro Perretti and Fulvio D'Acquisto

Blood (print ISSN 0006-4971, online ISSN 1528-0020), is published weekly by the American Society of Hematology, 2021 L St, NW, Suite 900, Washington DC 20036.